Optimized-Goppa Codes Based on the Effective Selection of Goppa Polynomials for Coded-Cooperative Generalized Spatial Modulation Network

Chen CHEN, Fengfan YANG, Daniel Kariuki WAWERU

College of Electronics and Information Engg., Nanjing Univ. of Aeronautics and Astronautics, Nanjing, 210016 China

chenchen05182020@163.com, yffee@nuaa.edu.cn, daniel.kariuki19@nuaa.edu.cn

Submitted September 18, 2023 / Accepted December 1, 2023 / Online first December 18, 2023

Abstract. *This paper proposes a novel optimized-Goppa-coded cooperative generalized spatial modulation (OGCC-GSM) scheme for short-to-medium information block transmission. In the proposed OGCC-GSM scheme, an efficient Goppa polynomial selection approach is designed to ensure that the selected Goppa codes applied in the source and relay nodes both have the largest minimum Hamming distance (MHD) and the optimal weight distribution. Compared to conventional coded cooperation (CC) with a single antenna, the proposed scheme employs the generalized spatial modulation (GSM) technique to achieve more diversity gains, where each node is equipped with multiple antennas and more than one transmit antenna (TA) is activated at each time-instant transmission. As a benchmark comparison, the OGCC spatial modulation (OGCC-SM) scheme is also investigated with a single TA active. Moreover, the reduced-complexity transmit antenna combination (RC-TAC) selection algorithm utilized in GSM is first developed with the aid of the channel state information (CSI) to reconcile computational complexity and system performance. In addition, joint decoding is conducted on the destination terminal to further enhance the performance of the proposed scheme. The simulated results indicate the performance of the proposed OGCC-GSM scheme is superior to that of its benchmark OGCC-SM scheme, with a substantial reduction in the number of TAs. Besides, Monte Carlo simulations demonstrate that the proposed OGCC-GSM scheme prevails over its counterparts by a margin of over 4.2 dB under identical conditions.*

Keywords

Optimized Goppa codes, Goppa polynomials, coded cooperation, generalized spatial modulation (GSM), spatial modulation (SM)

1. Introduction

In wireless communication systems, channel fading has been proven to deleteriously impair overall performance due to multipath propagation. The diversity technique is one of the most effective techniques to combat fading, which increases the reliability of the communication system by providing multiple remediable transmission paths that fade independently [1]. Currently, a relatively new diversity technique called user-cooperative diversity has emerged, which intelligently leverages path diversity. The fundamental concept of user cooperation is to share the whole/part information with at least two mobile users (source and relay) and transmit it with a single antenna to the common terminal (destination). Among the existing cooperative diversity techniques, coded cooperation (CC), combining channel coding and path diversity, demonstrates a superior bit error rate (BER) performance that offers both coding gain and diversity gain [2]. Many binary long channel codes including turbo-codes [3], polar codes [4], and low-density parity-check (LDPC) codes [5] have been deployed in CC. Recently, short-length non-binary codes have also been commonly utilized in CC to facilitate the transmission of small information blocks, such as for developing cellular and sensor networks [6]. Guo et al. [7] proposed the non-binary Reed Solomon coded cooperative (RSCC) scheme where two selection approaches are developed in the relay node to generate a strong final code in the destination node. As a maximum distance separable (MDS) code, the RS code has a great capacity to rectify random burst errors. Unfortunately, its information dimension and code length are conditional, limiting the proposed RSCC system from being generalizable. The focus then turns to another short-to-medium length code, namely Goppa code, which allows for more flexibility in selecting the code length and dimension, and has a low encoding and decoding complexity [8]. Clearly, the Goppa code is more appropriate to be implemented in practical engineering. Waweru et al. [9] and Feng et al. [10] both proposed the classic binary Goppa-coded cooperation (GCC) scheme. They employed relay selection methods similar to that in [7] to acquire a resultant code with superior weight distribution. However, the complexity of the two selection approaches is extremely high. To avoid the complexity induced by the selection without affecting the overall performance, we have opted to transfer all the

DOI: 10.13164/re.2024.0075

source's messages to the relay in this manuscript. In addition, two factors are required for the construction of a Goppa code: the code locator set and the Goppa polynomial. Under the premise of a given locator set, different Goppa polynomials may influence the performance of a Goppa code. In literature [9] and [10], the Goppa polynomial is selected randomly, ignoring this issue. Therefore, this paper proposes a simple but effective optimization selection approach for determining the optimum Goppa polynomial to achieve the Goppa code with the maximum free/minimum Hamming distance (FHD/MHD). And two optimized Goppa codes are employed in the CC to construct an optimized-Goppa-coded cooperative (OGCC) scheme.

Typically, coded cooperation is equipped with a single antenna at each node, resulting in low spectrum efficiency. Moreover, only binary-phase shift-keying (BPSK) modulation was considered in the previous GCC systems, which leads to poor bandwidth efficiency. Compared to single-antenna systems, multiple-input multiple-output (MIMO) systems are acknowledged to be a vital technology to enhance link reliability and spectrum efficiency [11]. Among many MIMO systems, spatial modulation (SM) may effectively avoid inter-channel interference (ICI) and inter-antenna synchronization (IAS) by conveying information with amplitude/phase modulated (APM) symbol and antenna index due to only one antenna being activated during a one-time instant transmission [12]. Hence, the total spectral efficiency increases by the base-two logarithms of the number of transmit antennas (TAs), implying that a large number of TAs is required to improve the spectral efficiency. To address this challenge, generalized spatial modulation (GSM) was proposed where more than one TA is activated concurrently to transmit a modulated symbol [13]. Consequently, for a certain spectrum efficiency, the number of TAs of GSM is lowered by more than half compared to SM. In the latest available literature [17], [18], the authors proposed distributed Goppa-coded spatial modulation (DGC-SM) and distributed Goppa-coded generalized spatial modulation (DGC-GSM) schemes, respectively, only adopting the relay selection approaches similar as ones developed by [9]. However, to our best knowledge, optimized Goppa codes by selecting Goppa polynomials have not been thoroughly investigated and implemented on CC. Inspired by this, the optimized-Goppa-coded cooperative GSM (OGCC-GSM) scheme is proposed as a fusion of the OGCC system and GSM technique in this manuscript. Moreover, its benchmark OGCC-SM system is presented as a counterpoint to the OGCC-GSM scheme. Note that not only one transmit antenna is selected in the GSM technique. Therefore, we also develop an appropriate transmit antenna combination (TAC) selection algorithm to optimize the activated antenna selection. Since the message at the relay node is dependent on that at the source, a joint decoding approach is established to obtain the final estimated messages.

Hence, the primary contributions of this paper are as below:

- An efficient selection approach of the Goppa polynomial is proposed to select an optimized Goppa code with the largest MHD and an optimal weight distribution.
- The novel OGCC-GSM scheme is proposed over the Rayleigh quasi-static fading channels where two optimized Goppa codes are utilized in the source and relay, respectively. And its benchmark OGCC-SM scheme is also developed as a comparison.
- Based on the optimum TAC algorithm [15], a reduced-complexity TAC (RC-TAC) selection algorithm is presented to maximize the minimum Euclidean distance (MED) of the transmitted signals using the channel state information (CSI).
- A joint decoding approach is developed for both OGCC-GSM and its benchmark OGCC-SM schemes to enhance the overall performance.
- The performance of the OGCC-GSM scheme is evaluated under the ideal and imperfect mobile user channels (source-to-relay links).

The remaining sections of the manuscript are structured as follows: Section 2 provides a concise overview of the Goppa code generation process and its fundamental properties. In Sec. 3, an optimized selection algorithm of the Goppa polynomials is proposed along with an example of the selection procedure. The OGCC-GSM scheme and the benchmark OGCC-SM scheme are presented over the Rayleigh fading channel in Sec. 4. Section 5 proposes a novel RC-TAC algorithm to trade off the complexity of the TAC selection and performance of the GSM. In Sec. 6, a joint decoding approach is developed in the destination. The various Monte-Carlo simulations are presented to validate the proposed OGCC-GSM scheme in Sec. 7. Ultimately the manuscript concludes with Sec. 8.

2. Fundamentals of Goppa Codes

Given the Galois field GF(2^m) (m is any positive integer), define the set $\mathcal{L} = \{\alpha_0, \alpha_1, \ldots \alpha_{N-1}\} \subset \mathrm{GF}(2^m)(\alpha_i \neq \alpha_j \text{ for } i \neq j)$ and a r-degree polynomial $\mathcal{G}(x) = x^r + \beta_0 x^{r-1} + \beta_1 x^{r-2} + \cdots + \beta_{r-1}$ ($\beta_k \in \mathrm{GF}(2^m), k = 0, 1, \ldots r-1$). Moreover, $\forall \alpha_i \in \mathcal{L}$, $\mathcal{G}(\alpha_i) \neq 0$. Then, a Goppa code $\Gamma(\mathcal{L}, \mathcal{G}(x))$ is determined as a (N, K, d) linear code where all components of the codeword $\mathbf{c} = \{c_0, c_1, \ldots, c_{N-1}\}$ are in GF(2) and satisfy the condition,

$$\sum_{i=0}^{N-1} \frac{c_i}{x - \alpha_i} \equiv 0 \mod \mathcal{G}(x). \tag{1}$$

It is noted that $\mathcal{L}$ is referred as the *code locator set*, and its cardinality determines the code length of $\Gamma(\mathcal{L}, \mathcal{G}(x))$, i.e., $|\mathcal{L}| = N$. Also, $\mathcal{G}(x)$ is recognized as the *Goppa polynomial* whose degree r also represents the number of rectifiable errors of this Goppa code. Generally, the MHD d satisfies $d \geq r + 1$ [9].

Furthermore, the parity-check matrix $\mathbf{H}$ of the Goppa code $\Gamma(\mathcal{L}, \mathcal{G}(x))$ for decoding is provided as

$$\mathbf{H} = \begin{bmatrix} \frac{1}{\mathcal{G}(\alpha_0)} & \frac{1}{\mathcal{G}(\alpha_1)} & \cdots & \frac{1}{\mathcal{G}(\alpha_{N-1})} \\ \frac{\alpha_0}{\mathcal{G}(\alpha_0)} & \frac{\alpha_1}{\mathcal{G}(\alpha_1)} & \cdots & \frac{\alpha_{N-1}}{\mathcal{G}(\alpha_{N-1})} \\ \frac{\alpha_0^2}{\mathcal{G}(\alpha_0)} & \frac{\alpha_1^2}{\mathcal{G}(\alpha_1)} & \cdots & \frac{\alpha_{N-1}^2}{\mathcal{G}(\alpha_{N-1})} \\ \vdots & \vdots & \cdots & \vdots \\ \frac{\alpha_0^{r-1}}{\mathcal{G}(\alpha_0)} & \frac{\alpha_1^{r-1}}{\mathcal{G}(\alpha_1)} & \cdots & \frac{\alpha_{N-1}^{r-1}}{\mathcal{G}(\alpha_{N-1})} \end{bmatrix}. \tag{2}$$

The dimension of the Goppa code $\Gamma(\mathcal{L}, \mathcal{G}(x))$ is $K \geq N - mr$. Each element in GF(2^m) corresponds to an m-bit vector. Therefore, $\mathbf{H}$ may need to extend to the $mr \times N$ binary matrix $\bar{\mathbf{H}}$, and then the systematic generator matrix $\mathbf{G}$ can be acquired by simple row transformation of $\bar{\mathbf{H}}$ for Goppa encoding.

Example: Given GF(2^4) and its primitive element β, take the loctor set $\mathcal{L} = \{1, \beta, \beta^2, \ldots, \beta^9\}$ and the Goppa polynomial $\mathcal{G}(x) = x + \beta^{12}$ (degree $r = 1$). Then, the Goppa code $\Gamma(\mathcal{L}, \mathcal{G}(x))$ is determined with the parameters $N = 10$, $K = 6$ and $d = 2$ (by computer exhaustive search). The parity-check matrix for this $\Gamma(\mathcal{L}, \mathcal{G}(x))$ is given as

$$\begin{aligned} \mathbf{H}_{1\times 10} &= \begin{bmatrix} \frac{1}{\mathcal{G}(1)} & \frac{1}{\mathcal{G}(\beta)} & \cdots & \frac{1}{\mathcal{G}(\beta^9)} \end{bmatrix} \\ &= [\beta^4, \beta^2, \beta^8, \beta^5, \beta^9, \beta, \beta^{11}, \beta^{13}, \beta^6, \beta^7]. \end{aligned} \tag{3}$$

Table 1 illustrates the corresponding 4-bit vector for each non-binary element in GF(2^4), and $\mathbf{H}$ is then extended into a 4×10 binary matrix $\bar{\mathbf{H}}$ as follows,

$$\bar{\mathbf{H}}_{4\times 10} = \begin{bmatrix} 1 & 0 & 1 & 0 & 0 & 0 & 0 & 1 & 0 & 1 \\ 1 & 0 & 0 & 1 & 1 & 1 & 1 & 0 & 1 & 1 \\ 0 & 1 & 1 & 1 & 0 & 0 & 1 & 1 & 1 & 0 \\ 0 & 0 & 0 & 0 & 1 & 0 & 1 & 1 & 0 & 1 \end{bmatrix}. \tag{4}$$

Moreover, the systematic generator matrix $\mathbf{G}$ of the Goppa code for encoding is obtained by row operations and transformation of $\bar{\mathbf{H}}$.

Field element	Vector	Field element	Vector
0	[0000]	$\beta^7 = 1 + \beta + \beta^3$	[1101]
1	[1000]	$\beta^8 = 1 + \beta^2$	[1010]
β	[0100]	$\beta^9 = \beta + \beta^3$	[0101]
β^2	[0010]	$\beta^{10} = 1 + \beta + \beta^2$	[1110]
β^3	[0001]	$\beta^{11} = \beta + \beta^2 + \beta^3$	[0111]
$\beta^4 = 1 + \beta$	[1100]	$\beta^{12} = 1 + \beta + \beta^2 + \beta^3$	[1111]
$\beta^5 = \beta + \beta^2$	[0110]	$\beta^{13} = 1 + \beta^2 + \beta^3$	[1011]
$\beta^6 = \beta^2 + \beta^3$	[0011]	$\beta^{14} = 1 + \beta^3$	[1001]

Tab. 1. The correspondence between the non-binary elements in GF(2^4) and the 4-bit vectors.

3. Optimized Selection of the Goppa Polynomial

Unlike MDS codes such as RS code whose minimum distance can reach $2r + 1$, the MHD d of Goppa code $\Gamma(\mathcal{L}, \mathcal{G}(x))$ has a low bound as $r + 1$. As the components of the code locator set $\mathcal{L}$ are selected independently and equitably from GF(2^m), $\mathcal{L} = \{\alpha_0, \alpha_1, \ldots \alpha_{N-1}\}$ is predetermined to meet the objective of controlling variables. Thus, the different selections of Goppa polynomials may result in various values of d. The unique Goppa polynomial is determined from 2^{mr} potential candidates. A random selection of $\mathcal{G}(x)$ may induce the error correction performance of a single Goppa code to be extremely poor. Hence, an efficient selection of $\mathcal{G}(x)$ for obtaining the maximum value max (d) and optimizing the weight distribution is essential.

3.1 Goppa Polynomial Selection Steps

Before presenting the design steps, the following terms are defined: 1) "$X \rightarrow Y$" signifies that event X that causes event Y; 2) $|A|$ denotes the cardinality of set A; 3) the weight distribution of $\Gamma(\mathcal{L}, \mathcal{G}(x))$ is provided as

$$W(x) = 1 + J_d x^d + J_{d+1} x^{d+1} + \cdots + J_N x^N \tag{5}$$

where J_q $(q = d, d + 1, ..., N)$ is the number of the codewords with the weight q. The specific steps of the optimized selection are outlined below:

Step 1 Determine the set Λ_0 to store the Goppa polynomials such that $\mathcal{G}(\alpha_i) \neq 0$ $(\forall \alpha_i \in \mathcal{L}, i = 0, 1, \ldots, N - 1)$ from all 2^{mr} candidates.

Step 2 Through the calculation or the computer search, some Goppa polynomials that lead the dimension of $\Gamma(\mathcal{L}, \mathcal{G}(x))$ to be more than K are removed, and the rest polynomials are kept in the set Λ_1.

Step 3 Traverse each $\mathcal{G}(x) \in \Lambda_1$, and exhaustively search for the d of each Goppa code $\Gamma(\mathcal{L}, \mathcal{G}(x))$ corresponding to $\mathcal{G}(x)$. Determine the value $w = \max(d)$, and the corresponding $\mathcal{G}(x) \rightarrow w$ are stored in set Λ_2. The value d in (6) is refreshed to w. If $|\Lambda_2| = 1$, proceed to Step 6. Otherwise, go to the next step.

Step 4 For each $\mathcal{G}(x) \in \Lambda_2$, determine J_w for each $\Gamma(\mathcal{L}, \mathcal{G}(x))$. Determine the minimum value $\delta_w = \min(J_w)$, and keep $\mathcal{G}(x) \rightarrow \delta_w$ in the set Ω_w. If $|\Omega_w| = 1$, J_w is updated to δ_w and skips to Step 6, else go to the next step.

Step 5 For each $\mathcal{G}(x) \in \Omega_w$, determine the number J_{w+1} of the codeword with weight $w + 1$ and $\delta_{w+1} = \min(J_{w+1})$. Refresh J_{w+1} as δ_{w+1} and $\mathcal{G}(x) \rightarrow \delta_{w+1}$ are stored in set Ω_{w+1}. If $|\Omega_{w+1}| \neq 1$, repeat Step 5 searching the codeword with weight adding 1 until N. Otherwise, come to the next step.

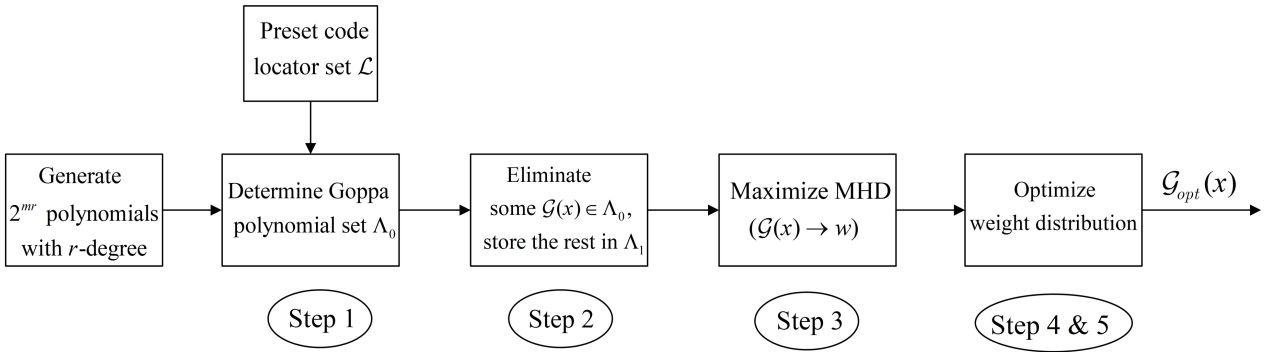

Fig. 1. Specific diagram of the Goppa polynomial selection.

Step 6 The optimum Goppa polynomial $\mathcal{G}_{\text{opt}}(x)$ is acquired and the selection approach is completed.

Note that if the selection procedure comes to acquiring J_N but $|\Omega_N| \neq 1$, $\mathcal{G}_{\text{opt}}(x)$ is selected randomly in set Ω_N. Moreover, the weight distribution $W(x)$ is also optimized by this selection approach. To make the proposed Goppa polynomial selection clearer, Figure 1 summarizes the effect of each step.

3.2 Selection Example

Given GF(2^4) and its primitive element β, the basic parameters of the $\Gamma(\mathcal{L}, \mathcal{G}(x))$ are set as $N = 14, K = 6$, and $r = 2$. To match N, predetermine $\mathcal{L} = \{1, \beta, \beta^2, ..., \beta^{13}\}$. Next, the selection process of the optimum Goppa polynomial $\mathcal{G}_{\text{opt}}(x)$ is provided as below:

Step 1 Since $r = 2$ and GF(2^4) are considered, determine the set Λ_0 to store all Goppa polynomials that satisfy the basic condition from 256 possible polynomials. By computer exhaustively search, the cardinality of Λ_0 is $|\Lambda_0| = 123$.

Step 2 From Λ_0, eliminate $\mathcal{G}(x) = x^2$ and $\mathcal{G}(x) = x^2 + \beta^{13}$ that both result in $K = 8 \neq 6$. The rest of the Goppa polynomials are kept in Λ_1. Thus, $|\Lambda_1| = 121$.

Step 3 For each $\mathcal{G}(x) \in \Lambda_1$, determine the d for the corresponding $\Gamma(\mathcal{L}, \mathcal{G}(x))$. Obtain $w = 5$ and all $\mathcal{G}(x) \to w$ are stored in Λ_2. The number of various values of d is displayed in Tab. 2. Since $|\Lambda_2| = 68 \neq 1$, and then come to the next step.

Step 4 For each $\mathcal{G}(x) \in \Lambda_2$, compute the number of codewords with the weight $w = 5$, and determine $\delta_5 = \min(J_5) = 10$, where the corresponding $\mathcal{G}(x)$ are saved in Ω_5. Since $|\Omega_5| = 23 \neq 1$, go to the next step.

Step 5 From Ω_5, continue to obtain $\delta_6 = \min(J_6) = 17$, and $|\Omega_6| = 6 \neq 1$. Then, $\delta_7 = \min(J_7) = 14$ are acquired from Ω_6 shown in Tab. 3. Since $|\Omega_7| = 1$, come to Step 6.

Step 6 The optimal $\mathcal{G}_{\text{opt}}(x) = x^2 + \beta^6 x + \beta^9$ is determined. The selection is finalized.

Value d	Number
2	2
3	16
4	35
5	68

d: the minimum free/Hamming distance of the Goppa code

Tab. 2. Quantitative statistics for different d values.

No.	$\mathcal{G}(x)$	w	δ_5	δ_6	J_7
1	$x^2 + \beta x + \beta^{11}$	5	10	17	16
2	$x^2 + \beta^2 x + \beta^3$	5	10	17	18
3	$x^2 + \beta^5 x + \beta^6$	5	10	17	17
4	$\boldsymbol{x^2 + \beta^6 x + \beta^9}$	**5**	**10**	**17**	**14**
5	$x^2 + \beta^8 x + \beta^4$	5	10	17	17
6	$x^2 + \beta^{11} x + \beta^{14}$	5	10	17	16

The row of the optimal Goppa polynomial is in bold.

Tab. 3. Six Goppa polynomials that result in w, δ_5, δ_6 and J_7.

This optimized selection approach ensures that a single Goppa code has the maximum MHD and as few codewords as possible have small weights. In this example, the weight distribution is optimized as

$$W(x) = 1 + 10x^5 + 17x^6 + 14x^7 + 10x^8 + 6x^9 + 3x^{10} + 2x^{11} + x^{12}. \quad (6)$$

4. Optimized-Goppa Coded Cooperative MIMO Schemes

4.1 The Proposed Model of the OGCC-GSM Scheme

Figure 2 displays the system structure of the proposed OGCC-GSM scheme with a single relay. Source and relay nodes in the OGCC-GSM scheme have the same numbers of antennas and activated TAs, designated as N_{t} and N_{a} ($N_{\text{a}} < N_{\text{t}}$), respectively, while the number of receive antennas (RAs) is represented as N_{r} at the destination node. Note that the relay node uses the same set of antennas to receive signals from the source and transmit signals to destination nodes, i.e., antenna multiplexing. However, the number of activated antennas is different in two phases after the inclusion of GSM technology. Furthermore, two Goppa codes

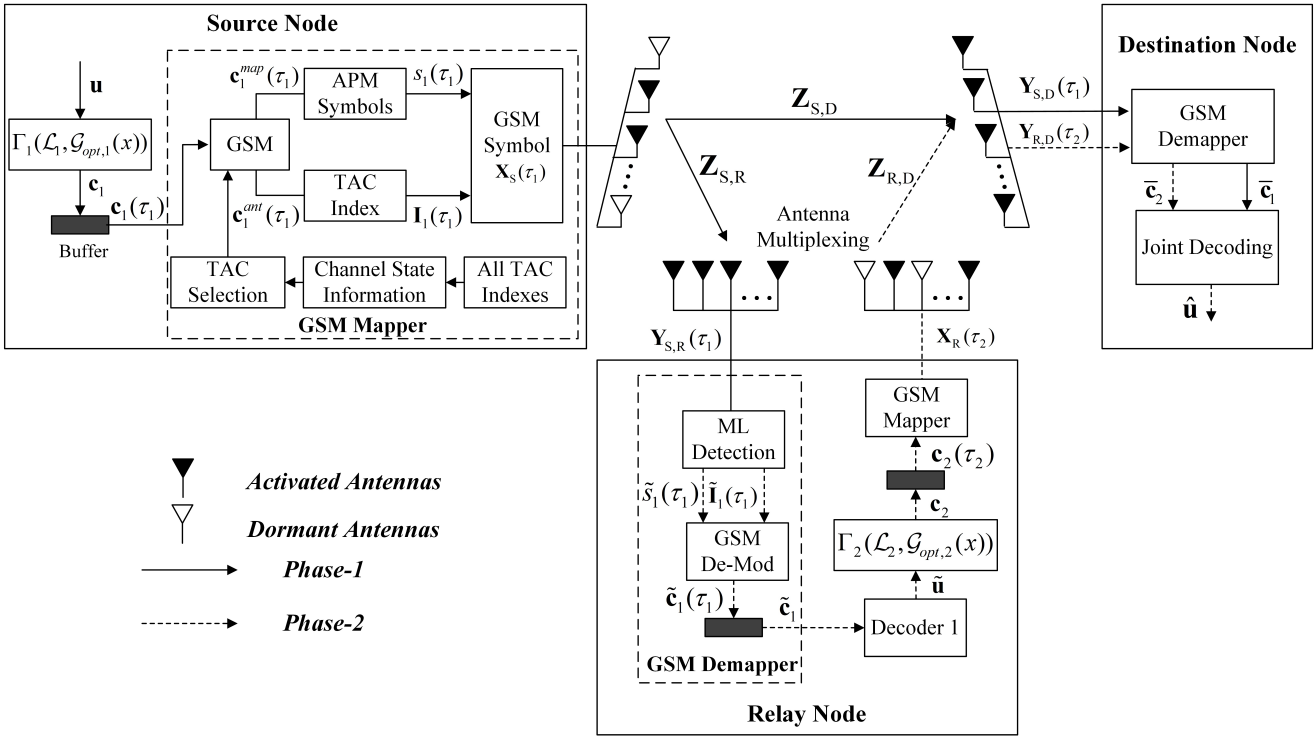

Fig. 2. Block diagram of the proposed half-duplex OGCC-GSM scheme.

from the same Galois field are optimized by the proposed selection approach and then distributed at the source and relay, respectively. The entire message transmission requires two phases to complete in a half-duplex manner.

During *phase-1*, the information bit sequence $\mathbf{u}$ is encoded by the optimized Goppa code $\Gamma_1(\mathcal{L}_1, \mathcal{G}_{\text{opt},1}(x))$ with code length N_1, code dimension K and the maximum MHD d_1 to obtain the encoded sequence $\mathbf{c}_1$. Through the buffer, $\mathbf{c}_1$ is split into the short sequences $\mathbf{c}_1(\tau_1)$ ($\tau_1 = 1, 2, \ldots, l_1, l_1 = (N_1 + N_1^{'})/n$) of length $n = \lfloor \log_2 \binom{N_t}{N_a} \rfloor + \log_2 M$, where $N_1^{'}$ is the number of dummy bits adding in $\mathbf{c}_1$ to ensure the length $(N_1 + N_1^{'})$ is a multiple of n, $\lfloor \cdot \rfloor$ represents the floor operation, and M stands for the modulation order. Then, all short sequences $\mathbf{c}_1(\tau_1)$ enter the 'GSM' module in turn, where first n_1-bits sequence $\mathbf{c}_1^{\text{ant}}(\tau_1)$ ($n_1 = \lfloor \log_2 \binom{N_t}{N_a} \rfloor$) is mapped to the activated TA indices $\mathbf{I}_1(\tau_1) = (I_1, I_2, \ldots, I_{N_a})$ in which $I_g \in \{1, 2, ..., N_t\}$ ($g = 1, 2, \ldots, N_a$) denotes the index of the activated TA referred to the selected TAC index table $\mathcal{I}_{\text{sel}}$ and the remaining bit vector $\mathbf{c}_1^{\text{map}}(\tau_1)$ of length $n_2 = \log_2 M$ is modulated as an M-PSK/QAM symbol $s_1(\tau_1)$. Combined with $\mathbf{I}_1(\tau_1)$ and $s_1(\tau_1)$, the $N_t \times 1$ GSM vector $\mathbf{X}_S(\tau_1)$ for each τ_1 at the source is given as

$$\mathbf{X}_S(\tau_1) = [\ldots, 0, s_1(\tau_1), 0, \ldots, 0, s_1(\tau_1), 0, \ldots]^T \quad (7)$$

where the modulated symbol $s_1(\tau_1)$ is only placed in the I_g-th TA ($I_g \in I_1(\tau_1), g = 1, 2, \ldots, N_a$) while other TAs keep dormant, and $[\cdot]^T$ is the transpose operation. Shown in the 'GSM Mapper' block of Fig. 2, the TAC index table is pre-selected based on the CSI that will be elaborated on in the next section. Subsequently, $\mathbf{X}_S(\tau_1)$ is broadcast simultaneously to the relay and destination nodes via the $N_r \times N_t$ MIMO Rayleigh quasi-static fading channels $\mathbf{Z}_{S,R}$ and $\mathbf{Z}_{S,D}$, respectively, whose elements are complex independent and identically distributed (i.i.d.) Gaussian random variables (RVs) following $\mathcal{CN}(0, 1)$. Note that $\mathbf{Z}_{S,R}$ and $\mathbf{Z}_{S,D}$ keep constant for each τ_1 while varying independently from one Goppa code to the next due to the Rayleigh quai-static fading. The received $N_r \times 1$ signal vectors $\mathbf{Y}_{S,R}(\tau_1)$ and $\mathbf{Y}_{S,D}(\tau_1)$ are formulated as

$$\begin{aligned} \mathbf{Y}_{S,R}(\tau_1) &= \mathbf{Z}_{S,R}\mathbf{X}_S(\tau_1) + \mathbf{N}_{S,R} \\ &= \sum_{g=1}^{N_a} \mathbf{z}_{I_g}^{S,R} s_1(\tau_1) + \mathbf{N}_{S,R}, \end{aligned} \quad (8)$$

$$\begin{aligned} \mathbf{Y}_{S,D}(\tau_1) &= \mathbf{Z}_{S,D}\mathbf{X}_S(\tau_1) + \mathbf{N}_{S,D} \\ &= \sum_{g=1}^{N_a} \mathbf{z}_{I_g}^{S,D} s_1(\tau_1) + \mathbf{N}_{S,D} \end{aligned} \quad (9)$$

where $\mathbf{z}_{I_g}^{S,R}$ represents the I_g-th column of $\mathbf{Z}_{S,R}$ that is the $N_r \times 1$ channel vector from the I_g-th activated TA at the source to all receive antennas at the relay. $\mathbf{z}_{I_g}^{S,D}$ is also defined similarly as $\mathbf{z}_{I_g}^{S,R}$. Moreover, $\mathbf{N}_{S,R}$ and $\mathbf{N}_{S,D}$ are the $N_r \times 1$ noise vectors from the source to the relay and destination nodes, yielding the complex Gaussian distribution as $\mathcal{CN}(0, \sigma^2)$ where σ^2 stands for the power spectral density (PSD) of noise.

During *phase-2*, supposing that the CSI is known at the relay, the optimal maximum likelihood (ML) detection is first performed on $\mathbf{Y}_{\mathrm{S,R}}(\tau_1)$, given as

$$\left[\tilde{\mathbf{I}}_1(\tau_1), \tilde{s}_1(\tau_1)\right] = \underset{\substack{\mathbf{I}_1(\tau_1)\in\mathcal{I}_{\mathrm{sel}} \\ s_1(\tau_1)\in\mathbb{S}}}{\arg\min} \left\| \mathbf{Y}_{\mathrm{S,R}}(\tau_1) - \sum_{g=1}^{N_{\mathrm{a}}} \mathbf{z}_{I_g}^{\mathrm{S,R}} s_1(\tau_1) \right\|_{\mathrm{F}}^2 \tag{10}$$

where $\mathbb{S}$ is the set of all signal constellation points and $\|\cdot\|_{\mathrm{F}}$ represents the Frobenius norm operation. Based on the selected TAC table $\mathcal{I}_{\mathrm{sel}}$ and the detected $\tilde{\mathbf{I}}_1(\tau_1), \tilde{s}_1(\tau_1)$, the estimated short sequence $\tilde{\mathbf{c}}_1(\tau_1)$ is obtained through 'GSM De-Mod' block. Again, via the buffer and the Decoder 1 of $\Gamma_1(\mathcal{L}_1, \mathcal{G}_{\mathrm{opt},1}(x))$, the entire estimated sequence $\tilde{\mathbf{c}}_1$ is decoded to recover the noise-corrupted message sequence $\tilde{\mathbf{u}}$. Notice that the 'ML Detection', 'GSM De-Mod', and the buffer blocks compose the 'GSM Dempper' module. Unlike the bit selection module ignoring some bits, $\tilde{\mathbf{u}}$ of length K is re-encoded by the other optimized-Goppa code $\Gamma_2(\mathcal{L}_2, \mathcal{G}_{\mathrm{opt},2}(x))$ with MHD d_2 to acquire N_2-length codeword $\mathbf{c}_2$. In general, $N_2 > N_1$ guarantees that the relay provides additional redundant bits. $\mathbf{c}_2$ is then divided into short sequence $\mathbf{c}_2(\tau_2)(\tau_2 = 1, 2, \ldots, l_2, l_2 = (N_2 + N_2^{'})/n)$, where $N_2^{'}$ is also the number of dummy bits defined similarly as $N_1^{'}$. Likewise, $\mathbf{c}_2(\tau_2)$ is sent to the 'GSM' module to attain the $N_{\mathrm{t}} \times 1$ GSM vector $\mathbf{X}_{\mathrm{R}}(\tau_2)$. The detailed process can be referred to $\mathbf{X}_{\mathrm{S}}(\tau_1)$ at the source node. Next, $\mathbf{X}_{\mathrm{R}}(\tau_2)$ is transmitted to the destination terminal, and the received signal vector $\mathbf{Y}_{\mathrm{R,D}}(\tau_2)$ is mathematically modeled as

$$\begin{aligned} \mathbf{Y}_{\mathrm{R,D}}(\tau_2) &= \mathbf{Z}_{\mathrm{R,D}}\mathbf{X}_{\mathrm{R}}(\tau_2) + \mathbf{N}_{\mathrm{R,D}} \\ &= \sum_{g=1}^{N_{\mathrm{a}}} \mathbf{z}_{I_g}^{\mathrm{R,D}} s_2(\tau_2) + \mathbf{N}_{\mathrm{R,D}} \end{aligned} \tag{11}$$

where $\mathbf{Z}_{\mathrm{R,D}}$ and $\mathbf{N}_{\mathrm{R,D}}$ are the Rayleigh quasi-static fading MIMO channel and the noise vector from the relay to the destination node, defined like $\mathbf{Z}_{\mathrm{S,R}}$ and $\mathbf{N}_{\mathrm{S,R}}$, respectively. Moreover, $\mathbf{z}_{I_g}^{\mathrm{R,D}}$ represents the I_g-th column of $\mathbf{Z}_{\mathrm{R,D}}$. Then, the received signals $\mathbf{Y}_{\mathrm{S,D}}(\tau_1)$ and $\mathbf{Y}_{\mathrm{R,D}}(\tau_2)$ are demodulated at the corresponding phase through 'GSM Demapper' block. Lastly, the 'Joint Decoding' block performs on the detected vectors $\bar{\mathbf{c}}_1$ and $\bar{\mathbf{c}}_2$ acquire to the estimated final information sequence $\hat{\mathbf{u}}$, which will be discussed in detail in Sec. 6.

4.2 Benchmark: OGCC-SM Scheme

The OGCC-SM scheme is introduced as a benchmark for the proposed OGCC-GSM scheme with the aid of Fig. 2. The primary distinction between SM and GSM is that only one TA is active in SM. Hence, the TAC selection is not required. More specifically, the modifications for the message transmission of the OGCC-SM scheme are discussed in detail below.

During the *phase-1*, the short sequence $\mathbf{c}_1(\bar{\tau}_1)$ $(\bar{\tau}_1 = 1, 2, \ldots, \bar{l}_1, \bar{l}_1 = (N_1 + \bar{N}_1^{'})/\bar{n})$ of length $\bar{n} = \log_2 N_{\mathrm{t}} + \log_2 M$ is also divided into two parts in SM: the first sequence $\mathbf{c}_1^{\mathrm{ant}}(\bar{\tau}_1)$ of length $\bar{n}_1 = \log_2 N_{\mathrm{t}}$ corresponds to one activated TA index $I_1(\bar{\tau}_1) \in \{1, 2, \ldots, N_{\mathrm{t}}\}$, and the rest n_2-bits sequence $\mathbf{c}_1^{\mathrm{map}}(\bar{\tau}_1)$ is modulated as an M-PSK/QAM symbol $s_1(\bar{\tau}_1)$ same as $\mathbf{c}_1^{\mathrm{map}}(\tau_1)$. This demonstrates a drawback of SM that the number of TA must be the power of 2 compared with GSM. Then, the $N_{\mathrm{t}} \times 1$ SM symbol vector $\mathbf{X}_{\mathrm{S}}(\bar{\tau}_1)$ for each $\bar{\tau}_1$ at the source node is written as

$$\mathbf{X}_{\mathrm{S}}(\bar{\tau}_1) = [\ldots, 0, s_1(\bar{\tau}_1), 0, \ldots]^{\mathrm{T}} \tag{12}$$

where $s_1(\bar{\tau}_1)$ is placed in the $I_1(\bar{\tau}_1)$-th TA. Likewise, the $N_{\mathrm{t}} \times 1$ SM symbol vector $\mathbf{X}_{\mathrm{R}}(\bar{\tau}_2)$ $(\bar{\tau}_2 = 1, 2, \ldots, \bar{l}_2, \bar{l}_2 = (N_2 + \bar{N}_2^{'})/\bar{n})$ at the relay node is acquired by the same process of the SM mapper of $\mathbf{X}_{\mathrm{S}}(\bar{\tau}_1)$ during the *phase-2*. The received signal vectors $\mathbf{Y}_{\mathrm{S,R}}(\bar{\tau}_1)$, $\mathbf{Y}_{\mathrm{S,D}}(\bar{\tau}_1)$ and $\mathbf{Y}_{\mathrm{R,D}}(\bar{\tau}_2)$ at the respective phase can refer to (8), (9), and (11). Furthermore, the joint decoding approach is applicable to the OGCC-SM scheme as well.

In both OGCC-GSM and OGCC-SM schemes, the code rate is $R_{\mathrm{CC}} = K/(N_1 + N_2)$ from the perspective of the destination node. Additionally, the spectral efficiency for the OGCC-GSM scheme is represented as $\lambda_{\mathrm{GSM}} = \lfloor \log_2 \binom{N_{\mathrm{t}}}{N_{\mathrm{a}}} \rfloor + \log_2 M$ while that for the OGCC-SM is denoted as $\lambda_{\mathrm{SM}} = \log_2 N_{\mathrm{t}} + \log_2 M$. Note that the OGCC-SM scheme requires more TAs than the OGCC-GSM scheme to achieve identical spectral efficiency.

5. Proposed RC-TAC Selection Algorithm Used in OGCC-GSM Scheme

For the OGCC-GSM scheme with N_{t} TAs and N_{a} activated TAs, $L = \binom{N_{\mathrm{t}}}{N_{\mathrm{a}}}$ valid TACs are available. However, only $L^{'} = 2^{\lfloor \log_2 \binom{N_{\mathrm{t}}}{N_{\mathrm{a}}} \rfloor}$ TACs are utilized to map the message bits in the 'GSM Mapper' block of the Fig. 2. Thus, there are $\binom{L}{L^{'}}$ potential TAC index tables that are all stored in the set $\mathbb{I}$, i.e.,

$$\mathbb{I} = \left\{ \mathcal{I}_b | b = 1, 2, ..., Q, Q = \binom{L}{L^{'}} \right\} \tag{13}$$

where $\mathcal{I}_b$ denotes the TAC index table. Evidently, $|\mathbb{I}| = Q$. Based on the CSI, Xiao el at. [15] proposed the optimum TAC selection algorithm that calculates all Euclidean distances (EDs) of different GSM vectors for each $\mathcal{I}_b$ to select one table with the maximum MED. Unfortunately, the computational complexity is extremely high considering the large values of N_{t} and N_{a}. Therefore, the RC-TAC selection algorithm is proposed to search the promising candidates based on the channel modulus sorting and the corresponding EDs, instead of searching all Q TAC index tables.

5.1 Algorithm Description

Taking the source-to-destination (S-D) transmission link as an example, the $N_\mathrm{r} \times N_\mathrm{t}$ CSI matrix $\mathbf{Z}_{\mathrm{S,D}} = [\mathbf{z}_1^{\mathrm{S,D}}, \mathbf{z}_2^{\mathrm{S,D}}, ..., \mathbf{z}_{N_\mathrm{t}}^{\mathrm{S,D}}]$ is known at the source where $\mathbf{z}_k^{\mathrm{S,D}} \in C^{N_\mathrm{r}\times 1}(k = 1, 2, ..., N_\mathrm{t})$ is the k-th column of $\mathbf{Z}_{\mathrm{S,D}}$. The specific selection algorithm includes six steps:

Step 1 Determine the set $\mathcal{Z}$ of the modulus of the N_t columns for $\mathbf{Z}_{\mathrm{S,D}}$, given as

$$\mathcal{Z} = \left\{ \left\| \mathbf{z}_1^{\mathrm{S,D}} \right\|_\mathrm{F}^2, \left\| \mathbf{z}_2^{\mathrm{S,D}} \right\|_\mathrm{F}^2, \ldots, \left\| \mathbf{z}_{N_\mathrm{t}}^{\mathrm{S,D}} \right\|_\mathrm{F}^2 \right\}. \tag{14}$$

Step 2 Sort $\mathcal{Z}$ in descending order with the corresponding TA index I_k is recorded sequentially and saved in the set Δ, where $\Delta = \{I_1, I_2, ..., I_{N_\mathrm{t}}\}$.

Step 3 Divide the sorted set Δ into two parts: first N_u indexes and the remaining $N_\mathrm{t} - N_\mathrm{u}$ indexes, stored in the Δ_1 and Δ_2, respectively, where $N_\mathrm{u} = \lceil \frac{N_\mathrm{t}+1}{2} \rceil$, and $\lceil \cdot \rceil$ represents the ceil operation.

Step 4 Perform a selection of prospective TAC index candidates. Preference is given to the indexes in the set Δ_1. To guarantee $L^{'}$ TACs, Δ_2 also need to be chosen. The total number $\bar{L}$ is obtained as

$$\begin{aligned} \bar{L} = \binom{N_\mathrm{u}}{N_\mathrm{a}} + \binom{N_\mathrm{u}}{N_\mathrm{a}-1}\binom{N_\mathrm{t}-N_\mathrm{u}}{1} + \cdots \\ + \binom{N_\mathrm{u}}{1}\binom{N_\mathrm{t}-N_\mathrm{u}}{N_\mathrm{a}-1}. \end{aligned} \tag{15}$$

Then, save all reduced TAC index tables $\mathcal{I}_{\bar{b}}, (\bar{b} = 1, 2, ..., \bar{Q})$ in the set $\bar{\mathbb{I}}$, where $|\bar{\mathbb{I}}| = \bar{Q}$, and $\bar{Q} = \binom{\bar{L}}{L'}$.

Step 5 For each table $\mathcal{I}_{\bar{b}}$, determine the MED $D_{\min}^{\bar{b}}$ by calculating the EDs between different GSM vectors $\mathbf{X}_{\mathrm{S},1}$ and $\mathbf{X}_{\mathrm{S},2}$ at the source node, as [15]

$$\begin{aligned} D_{\min}^{\bar{b}} &= \min_{\mathbf{X}_{\mathrm{S},1} \neq \mathbf{X}_{\mathrm{S},2}} \left\| \mathbf{Z}_{\mathrm{S,D}}\mathbf{X}_{\mathrm{S},1} - \mathbf{Z}_{\mathrm{S,D}}\mathbf{X}_{\mathrm{S},2} \right\|_\mathrm{F}^2 \\ &= \min_{\substack{s_{1,1} \neq s_{1,2} \in \mathbb{S} \\ \mathbf{I}_{1,1} \neq \mathbf{I}_{1,2} \in \mathcal{I}_{\bar{b}}}} \left\| \sum_{g=1}^{N_\mathrm{a}} (\mathbf{z}_{I_{g,1}}^{\mathrm{S,D}} s_{1,1} - \mathbf{z}_{I_{g,2}}^{\mathrm{S,D}} s_{1,2}) \right\|_\mathrm{F}^2 \end{aligned} \tag{16}$$

where $I_{g,j}(j = 1, 2)$ denotes the index in the a single TAC $\mathbf{I}_{1,j}$.

Step 6 Obtain the TAC index table $\mathcal{I}_{\mathrm{sel}}$ with a maximum $D_{\min}^{\bar{b}}$ given as

$$\mathcal{I}_{\mathrm{sel}} = \arg \max_{\mathcal{I}_{\bar{b}} \in \bar{\mathbb{I}}} (D_{\min}^{\bar{b}}). \tag{17}$$

And, the selection is terminated.

Note that in Step 3, Δ_1 is viewed as the set of promising index candidates due to the large value of channel modulus. Thus, N_a activated TA is selected first in the set Δ_1. Then, incremental selections are made from the alternate index set Δ_2 to ensure $L^{'}$ different information vectors can be mapped one by one.

5.2 Complexity Analysis

In this manuscript, the measure of computational complexity is the number of floating-point operations (Flops), where a Flop represents a real-valued addition or multiplication operation. There are two components to the computational complexity of the proposed RC-TAC algorithm: the calculation of the channel modulus shown in (14) and the computation of the various EDs in (16). For the channel modulus, the single operation $\left\| \mathbf{z}_k^{\mathrm{S,D}} \right\|_\mathrm{F}^2 (k = 1, 2, ..., N_\mathrm{t})$ requires $4N_\mathrm{r} - 1$ Flops. Thereby, the number of the Flops for N_t channel modulus operations is $C_1 = 4N_\mathrm{t}N_\mathrm{r} - N_\mathrm{t}$. Searching the MED in single table $\mathcal{I}_{\bar{b}}$ needs $7N_\mathrm{a}N_\mathrm{r}M(4N_\mathrm{r} - 1)(M - 1)$ Flops. Since all $\bar{Q}$ tables are searched, the complexity C_2 for determining the maximum MED is $C_2 = 7N_\mathrm{a}N_\mathrm{r}M\bar{Q}(4N_\mathrm{r} - 1)(M - 1)$. Hence, the total Flops C_RC of the proposed RC-TAC selection is given as

$$\begin{aligned} C_\mathrm{RC} &= C_1 + C_2 \\ &= 4N_\mathrm{t}N_\mathrm{r} - N_\mathrm{t} + 7N_\mathrm{a}N_\mathrm{r}M\bar{Q}(4N_\mathrm{r} - 1)(M - 1). \end{aligned} \tag{18}$$

Furthermore, the optimum TAC selection has the following complexity, given as

$$C_\mathrm{opt} = 7N_\mathrm{a}N_\mathrm{r}MQ(4N_\mathrm{r} - 1)(M - 1). \tag{19}$$

For a more intuitive presentation, Table 4 compares the complexity of two selection algorithms by several groups of MIMO configurations. Compared to the optimal TAC selection, the proposed RC-TAC selection algorithm shows a dramatic reduction in complexity. When the values N_t and N_a are large, the advantage of the proposed RC-TAC algorithm becomes more apparent, and $\mathcal{I}_{\mathrm{sel}}$ may be selected more quickly.

MIMO configurations $M = 4, N_\mathrm{r} = 5$	Search volume		Complexity [Flops]		Percentage reduction [%]
	Q	$\bar{Q}$	C_opt	C_RC	
$N_\mathrm{t} = 5, N_\mathrm{a} = 2, L = 10, L^{'} = 8, \bar{L} = 9$	45	9	718200	143735	79.9
$N_\mathrm{t} = 6, N_\mathrm{a} = 2, L = 15, L^{'} = 8, \bar{L} = 14$	6435	3003	102702600	47927994	53.3
$N_\mathrm{t} = 7, N_\mathrm{a} = 3, L = 35, L^{'} = 32, \bar{L} = 34$	6545	561	156687300	13430473	91.4

Tab. 4. The computational complexity comparison of the two selection algorithms.

6. Joint Decoding for the Proposed Schemes

To maximize the utilization of the two signals at the destination, and then enhance the system performance of the proposed OGCC-GSM and its benchmark OGCC-SM schemes, we propose a joint decoding approach. The flowchart can make reference to the 'Joint Goppa Decoding' block in Fig. 3 and the concrete steps are outlined below,

Step 1 The detected vector $\bar{\mathbf{c}}_2$ is first sent to the 'Decoder 2' of the optimized-Goppa code $\Gamma_2(\mathcal{L}_2, \mathcal{G}_{\text{opt},2}(x))$ to attain the estimated information sequence $\bar{\mathbf{u}}$ from the relay.

Step 2 Through the 'Combiner' block, substitute the last K information bits in the systematic vector $\bar{\mathbf{c}}_1$ with the newly acquired bits $\bar{\mathbf{u}}$, while maintaining the initial first $N_1 - K$ parity-check bits $\mathbf{p}_1$ of $\bar{\mathbf{c}}_1$. The mixed codeword $\hat{\mathbf{c}}_1$ is generated as $\hat{\mathbf{c}}_1 = [\mathbf{p}_1, \bar{\mathbf{u}}]$.

Step 3 Transmit $\hat{\mathbf{c}}_1$ to the 'Decoder 1' of the optimized-Goppa code $\Gamma_1(\mathcal{L}_1, \mathcal{G}_{\text{opt},1}(x))$ to obtain the estimated final message sequence $\hat{\mathbf{u}}_1$.

Note that 'joint' is embodied in Step 2 where the information bits in the relay are jointly used in the sequence at the source node. It is because the relay is positioned closer to the destination than the source in CC, resulting in more SNR gains. In addition, $\Gamma_2(\mathcal{L}_2, \mathcal{G}_{\text{opt},2}(x))$ at the relay contains more redundant bits, the detected information sequence $\bar{\mathbf{u}}$ is more reliable, and it is therefore totally utilized in the $\hat{\mathbf{c}}_1$. Furthermore, Patterson algorithm [14] is applied in 'Decoder 1' and 'Decoder 2' blocks demonstrating a stronger error correction capability than the existing Euclidean algorithm [9], [10], which is verified in the next simulation section.

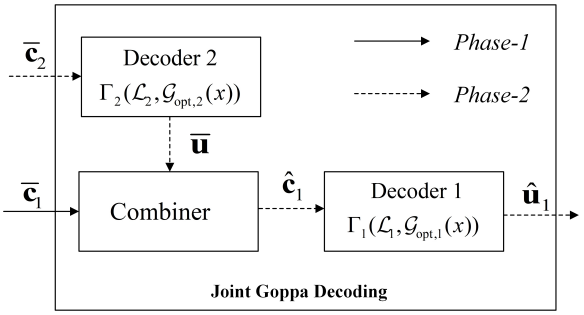

Fig. 3. The schematic diagram of the proposed joint decoding.

7. Simulation

In this section, Monte Carlo simulation results for analyzing the BER performance of the proposed OGCC-GSM scheme and other comparison schemes with the joint decoding over Rayleigh quasi-static fading channels are presented, where the number of simulated iterations reaches 10^5. To generalize and evaluate the OGCC-GSM scheme more comprehensively, Goppa codes used in the proposed scheme are randomly chosen from three distinct fields, i.e., GF(2^4), GF(2^5) and GF(2^6), where β, α and γ denote the primitive elements in respective Galois fields. The specific simulated parameters are summarized in Tab. 5, where different code rates ($R_{\text{CC}} = 1/4, 2/9$, and $1/3$) are considered for three scenarios. Define $\Upsilon_{\text{S,D}}$, $\Upsilon_{\text{S,R}}$, and $\Upsilon_{\text{R,D}}$ stand for the signal noise ratio (SNR) per bit from the direct S-D, S-R, and R-D transmission links, respectively. Assume a 2 dB SNR enhancement at the relay compared to the source, i.e. $\Upsilon_{\text{R,D}} = \Upsilon_{\text{S,D}} + 2$ dB, and perfect CSI at all related receivers for the GSM detection.

7.1 BER Performance for the GCC-GSM Schemes Under Various Goppa Polynomials

Based on the proposed efficient selection approach for the optimum Goppa polynomials in Sec. 3, Table 6 provides multiple typical Goppa polynomials for the Goppa codes to exhibit several kinds of search results, including the optimal $\mathcal{G}_{\text{opt},1}(x)$ and $\mathcal{G}_{\text{opt},2}(x)$ under three scenarios as well as a few groups of random Goppa polynomials. The corresponding MHD d_1 and d_2 are also presented in Tab. 6, where the number of the codewords with the weight equal to the maximum d_1 and d_2, i.e., $J_{\max(d_1)}, J_{\max(d_2)}$, are also contained. The specific selection procedure can be referred to in Sec. 3.2. As the search code space and the number of correctable errors are large, it is discovered that the optimal Goppa polynomial may be uniquely determined only by obtaining the minimum value of $J_{\max(d_1)}$ and $J_{\max(d_2)}$ for the source and relay, respectively, referring to the parameters in Scenarios 2 and 3 of Tab. 6.

Figures 4–6 demonstrate the BER performance of the GCC-GSM schemes for three scenarios to compare the influence of different Goppa polynomials, where $N_{\text{r}} = N_{\text{t}}$. Besides, the ideal source-to-relay transmission link ($\Upsilon_{\text{S,R}} = \infty$) and optimum TAC index table are applied in all three scenarios. From the simulated results, the GCC-GSM scheme using the optimal Goppa polynomials, i.e., OGCC-GSM scheme,

Scenario	Galois field	Source Goppa coding	Relay Goppa coding	R_{CC}	MIMO configurations
1	GF(2^4)	$N_1 = 10, K = 6, r_1 = 1$ $\mathcal{L}_1 = \{1, \beta, \beta^2, \ldots, \beta^9\}$	$N_2 = 14, K = 6, r_1 = 2$ $\mathcal{L}_2 = \{1, \beta, \beta^2, ..., \beta^{13}\}$	1/4	$N_{\text{t}} = 4, N_{\text{a}} = 2$ $N_{\text{r}} = 4, M = 2$
2	GF(2^5)	$N_1 = 22, K = 12, r_1 = 2$ $\mathcal{L}_1 = \{1, \alpha, \alpha^2, \ldots, \alpha^{21}\}$	$N_2 = 27, K = 12, r_1 = 3$ $\mathcal{L}_2 = \{1, \alpha, \alpha^2, ..., \alpha^{26}\}$	2/9	$N_{\text{t}} = 5, N_{\text{a}} = 2$ $N_{\text{r}} = 5, M = 4$
3	GF(2^6)	$N_1 = 30, K = 24, r_1 = 1$ $\mathcal{L}_1 = \{1, \gamma, \gamma^2, \ldots, \gamma^{29}\}$	$N_2 = 42, K = 24, r_1 = 3$ $\mathcal{L}_2 = \{1, \gamma, \gamma^2, ..., \gamma^{41}\}$	1/3	$N_{\text{t}} = 7, N_{\text{a}} = 3$ $N_{\text{r}} = 7, M = 16$

Tab. 5. Specific simulation parameters.

exhibits a prominent performance gain over the original GCC-GSM schemes employing the random Goppa polynomials. For example, the OGCC-GSM scheme of Scenario 1 achieves the SNR gain of over 3.5 dB at BER = 3×10^{-6}.

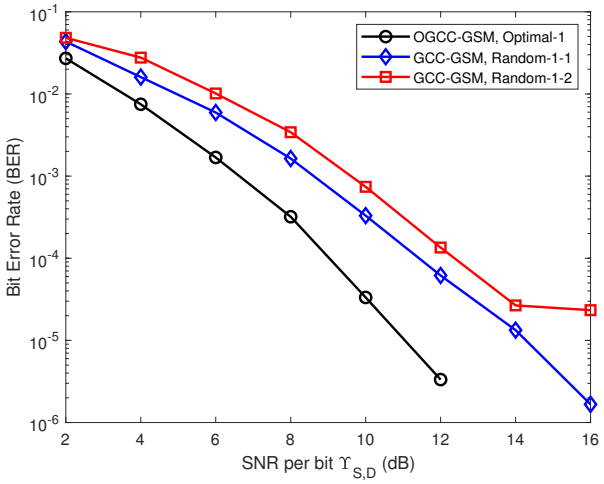

Fig. 4. Performance of the GCC-GSM schemes with $N_r = N_t = 4$ and BPSK modulation under different Goppa polynomials for Scenario 1.

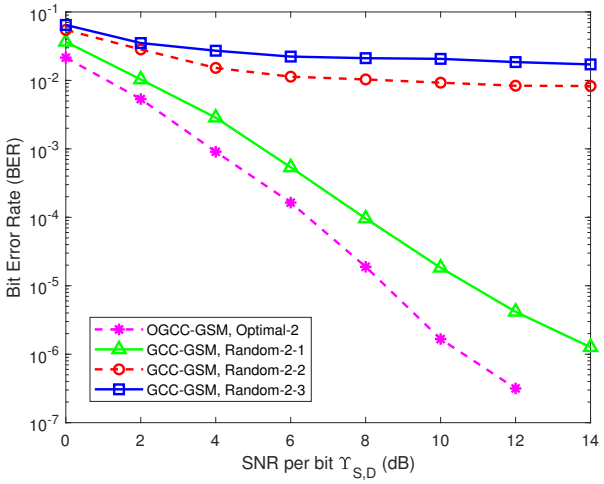

Fig. 5. Performance of the GCC-GSM schemes with $N_r = N_t = 5$ and 4-QAM under different Goppa polynomials for Scenario 2.

Moreover, randomly selected Goppa polynomials may make the MHDs of Goppa codes utilized in the source and relay nodes very small, resulting in the occurrence of the error floor (EF) region and poor overall system performance, as shown in Scenarios 2 and 3 of Figs. 5 and 6. Additionally, the different $J_{\max(d_1)}$ and $J_{\max(d_2)}$ also affect BER performance, even if the Goppa codes with the random and optimal polynomials used have the same MHD. Clearly, the fewer codewords with a small weight, the stronger the error correction capability of the code, which is also confirmed by the simulation results. For instance, the OGCC-GSM scheme of Scenario 2 outperforms the GCC-GSM schemes using the polynomial Random-2-1 by a gain over 3.5 dB at BER = 1.3×10^{-6}, where the same MHDs are selected at the source and relay for the fair comparison. In conclusion, the proposed effective Goppa polynomial selection algorithm has a substantial effect on the performance of the GCC-GSM, further indicating the necessity to propose the OGCC-GSM scheme. The optimal polynomials used in the OGCC-GSM scheme for the three scenarios in the simulations below are referred to in bold in Tab. 6 and are no longer specified.

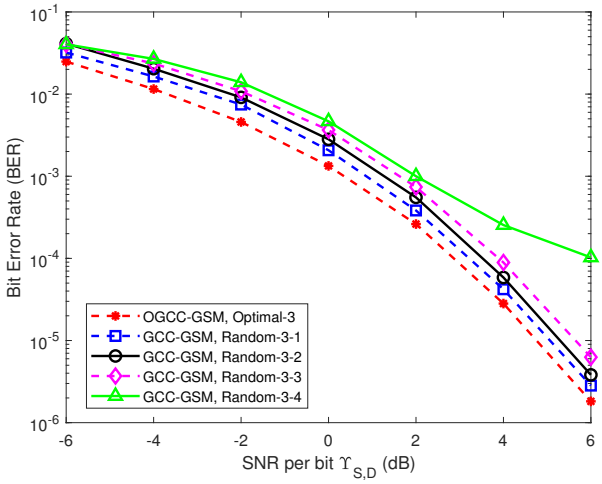

Fig. 6. Performance of the GCC-GSM schemes with $N_r = N_t = 7$ and 16-QAM under different Goppa polynomials for Scenario 3.

Scenario	Kind	$\mathcal{G}_1(x)$	d_1	$J_{\max(d_1)}$	$\mathcal{G}_2(x)$	d_2	$J_{\max(d_2)}$
1	Optimal-1	$\boldsymbol{x}$	3	9	$\boldsymbol{x^2+\beta^6 x+\beta^9}$	5	10
	Random-1-1	$x+\beta^{10}$	3	9	$x^2+x+\beta^{11}$	4	-
	Random-1-2	$x+\beta^{12}$	2	-	$x^2+\beta^5 x+\beta^{13}$	3	-
2	Optimal-2	$\boldsymbol{x^2+\alpha^{22}x+\alpha^{16}}$	5	22	$\boldsymbol{x^3+\alpha^3 x^2+\alpha^{28}x+\alpha^{10}}$	7	17
	Random-2-1	$x^2+x+\alpha^{12}$	5	37	$x^3+\alpha^4 x+\alpha^{13}$	7	35
	Random-2-2	$x^2+\alpha^7 x+\alpha^{26}$	4	-	$x^3+\alpha^5 x^2+\alpha^{11}x+\alpha^{24}$	6	-
	Random-2-3	$x^2+\alpha^{12}x+\alpha^{10}$	3	-	$x^3+\alpha^{20}x^2+\alpha^5 x+\alpha^{12}$	5	-
3	Optimal-3	$\boldsymbol{x+\gamma^{43}}$	3	47	$\boldsymbol{x^3+\gamma^{56}x+\gamma^{53}}$	7	56
	Random-3-1	$x+\gamma^{49}$	3	48	$x^3+\gamma x^2+\gamma^{25}x+\gamma^{33}$	7	82
	Random-3-2	x	3	53	$x^3+\gamma^2 x^2+\gamma^5 x+\gamma^{23}$	7	97
	Random-3-3	$x+\gamma^{30}$	3	60	$x^3+\gamma^{34}x+\gamma^{15}$	6	-
	Random-3-4	$x+\gamma^{28}$	2	-	$x^3+\gamma^2 x^2+\gamma^{53}x+\gamma^{42}$	5	-

The optimal polynomials of the OGCC-GSM scheme under three scenarios are in bold.

Tab. 6. Different Goppa polynomials for three simulated scenarios and the corresponding MHDs.

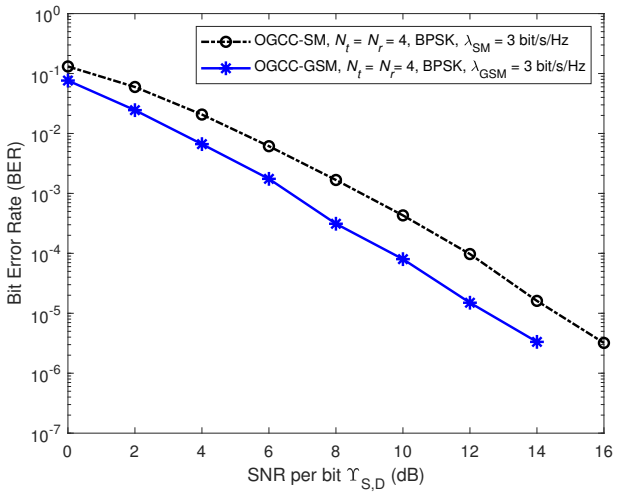

Fig. 7. BER performance comparison of the OGCC-GSM scheme and corresponding OGCC-SM scheme for Scenario 1.

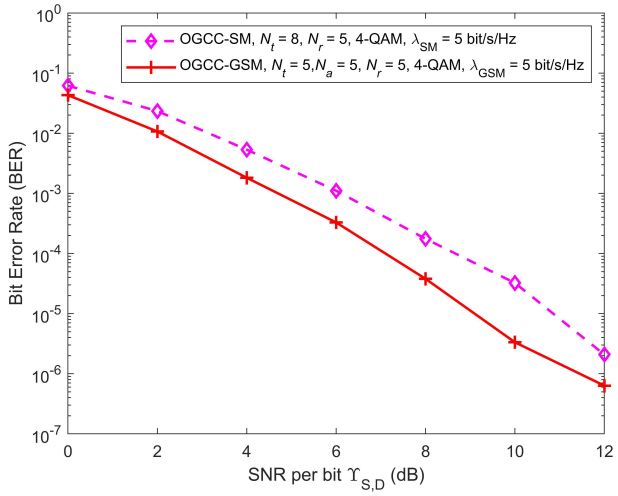

Fig. 8. BER performance comparison of the OGCC-GSM scheme and corresponding OGCC-SM scheme for Scenario 2.

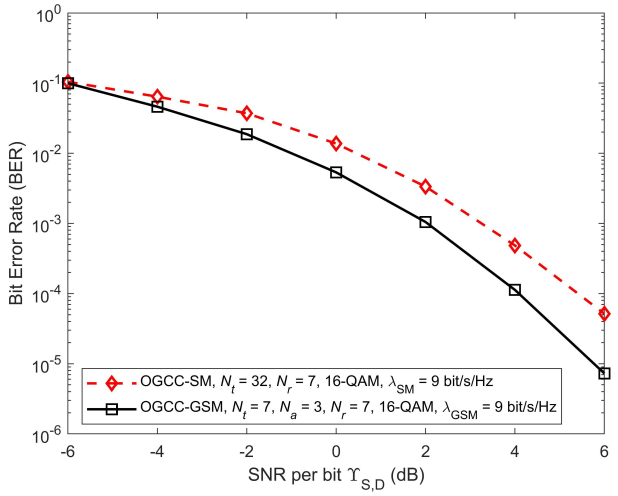

Fig. 9. BER performance comparison of the OGCC-GSM scheme and corresponding OGCC-SM scheme for Scenario 3.

Scenario	Spectral efficiency ($\lambda_{SM} = \lambda_{GSM}$)	OGCC-GSM	OGCC-SM
1	3 bits/s/Hz	$N_t = 4$, $N_a = 2$ $N_r = 4$ $M = 2$	$N_t = 4$ $N_r = 4$ $M = 2$
2	5 bits/s/Hz	$N_t = 5$, $N_a = 2$ $N_r = 5$ $M = 4$	$N_t = 8$ $N_r = 5$ $M = 4$
3	9 bits/s/Hz	$N_t = 7$, $N_a = 3$ $N_r = 7$ $M = 16$	$N_t = 32$ $N_r = 7$ $M = 16$

Tab. 7. MIMO configurations for the OGCC-GSM and OGCC-SM schemes with the identical spectral efficiencies corresponding to three scenarios.

7.2 Performance of the OGCC-GSM Scheme Versus that of its Benchmark OGCC-SM Scheme

This subsection discusses the performance comparisons between the proposed OGCC-GSM scheme under the optimum TAC index table and the corresponding benchmark scheme for all three scenarios. Likewise, assume $\Upsilon_{S,R} = \infty$. Since the spectral efficiencies of the proposed OGCC-GSM scheme for three scenarios are $\lambda_{GSM} = 3, 5, 9$ bits/s/Hz, respectively, the spectral efficiencies of the benchmark OGCC-SM scheme must be set to match that of the OGCC-GSM scheme for an equitable comparison, i.e., $\lambda_{SM} = \lambda_{GSM}$. Table 7 details the different numbers of TAs utilized by the OGCC-GSM and OGCC-SM schemes to attain identical spectral efficiency, including the required values N_r and M for each scenario.

The performance comparison results of the OGCC-GSM and OGCC-SM schemes under the three scenarios are presented in Figs. 7–9. From Fig. 7, the OGCC-GSM scheme can achieve a gain of 2 dB at BER $\approx 3.3 \times 10^{-6}$ compared to the benchmark OGCC-SM scheme in Scenario 1. Meanwhile, the OGCC-GSM scheme performs better than the OGCC-SM scheme with a margin of approximately 1.8 dB at BER $\approx 2.2 \times 10^{-6}$ under Scenario 2 (exhibited in Fig. 8) and 1.5 dB at BER $\approx 5 \times 10^{-5}$ under Scenario 3 (shown in Fig. 9), respectively. Consequently, the proposed OGCC-GSM is more applicable to engineering scenarios due to a substantial reduction in the number of TAs and a superior system performance compared to its benchmark OGCC-SM scheme.

7.3 Performance Comparison for the OGCC-GSM Employing Different TAC Selections

Figures 10–12 provide the BER performance of the OGCC-GSM scheme for three scenarios under the optimal TAC, RC-TAC, and random TAC selections, where $\Upsilon_{S,R} = \infty$, $N_r = N_t$ are supposed in the simulations. For Scenario 1 of Fig. 10, the optimal TAC selection is equivalent to RC-TAC selection owing to the same search volume ($Q = \bar{Q} = 15$). Thereby, the OGCC-GSM scheme exhibits virtually identical performance under two distinct selection algorithms. Moreover, due to a small search volume,

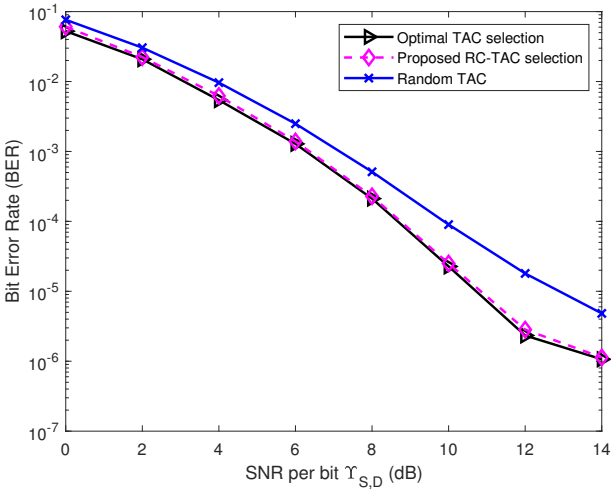

Fig. 10. Performance comparison of the OGCC-GSM scheme with $N_t = 4$, $N_a = 2$ under different TAC selection algorithms for Scenario 1.

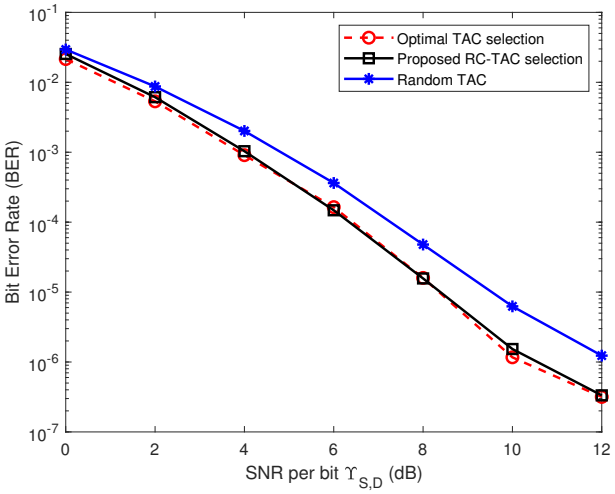

Fig. 11. Performance comparison of the OGCC-GSM scheme with $N_t = 5$, $N_a = 2$ under different TAC selection algorithms for Scenario 2.

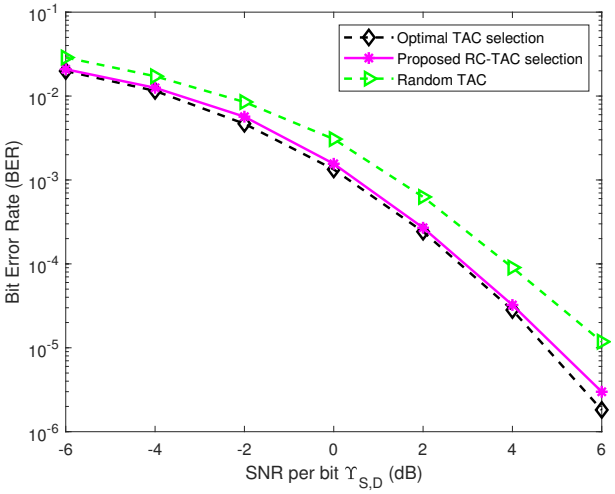

Fig. 12. Performance comparison of the OGCC-GSM scheme with $N_t = 7$, $N_a = 3$ under different TAC selection algorithms for Scenario 3.

the RC-TAC selection algorithm may pick out the same TAC index table as the optimal TAC selection algorithm, resulting in a nearly identical system performance, as depicted in Scenario 2 of Fig. 11. When the search volume is large as in Scenario 3 ($Q = 6545, \bar{Q} = 561$; see Tab. 4), the OGCC-GSM scheme under the proposed RC-TAC selection algorithm also demonstrates promising performance, with an SNR loss of only 0.6 dB compared to the scheme using the optimal selection at BER = 1.4×10^{-6}.

From Figs. 10–12, the OGCC-GSM scheme under the proposed RC-TAC selection algorithm for three scenarios performs significantly better than that under the random TAC table. For example, a performance gain of 2 dB is acquired at BER $\approx 10^{-6}$ for the OGCC-GSM under the RC-TAC selection compared to the random TAC table, while nearly no SNR loss compared to the scheme using the optimal TAC selection that requires large computational complexity, shown in Scenario 2 of Fig. 11. This indicates that the RC-TAC selection algorithm may provide a superior compromise between the search complexity and BER performance.

7.4 BER Performance Comparison of the OGCC-GSM Scheme Between the Practical and Ideal S-R Transmission Channels and its Non-Cooperative Scheme

All of the aforementioned simulations assume that the information between mobile users is accurately obtained, i.e., that the S-R transmission channel is ideal ($\Upsilon_{S,R} = \infty$), so as to achieve the purpose of controlling variables and ensure that more attention is paid to experimental parameters that need to be compared, such as the influence of different polynomials in Sec. 7.1 on the proposed OGCC-GSM scheme, for more objective and unbiased results. Nevertheless, information transfer between users may not be ideal in actual situations. To make the proposed OGCC-GSM scheme more applicable, it is necessary to evaluate its efficacy under non-ideal conditions.

Hence, we present the performance comparisons for the OGCC-GSM scheme with the RC-TAC selection algorithm under multiple S-R transmission link states including the practical ($\Upsilon_{S,R} \neq \infty$) and ideal ($\Upsilon_{S,R} = \infty$) links for three scenarios in Figs. 13–15. In Scenario 1, $\Upsilon_{S,R} = 8, 14$ dBs are considered as the practical links. Besides, the non-ideal channels $\Upsilon_{S,R} = 5, 12$ dBs are preset for Scenario 2, and $\Upsilon_{S,R} = 3, 10$ dBs are evaluated in Scenario 3, respectively. It is observed that the OGCC-GSM scheme for three scenarios under the poor S-R channels, i.e., $\Upsilon_{S,R} = 8$, 5, and 3 dBs, respectively, demonstrates an approximative BER performance compared to the OGCC-GSM scheme under $\Upsilon_{S,R} = \infty$ at low SNR. However, at high SNR, the EF region occurs and the performance significantly deteriorates due to uncontrolled error propagation, which can be mitigated by the cyclic redundancy check (CRC) approach [16]. In addition, in the case of a robust S-R link, the OGCC-GSM scheme for three scenarios exhibits nearly identical BER performance as the ideal

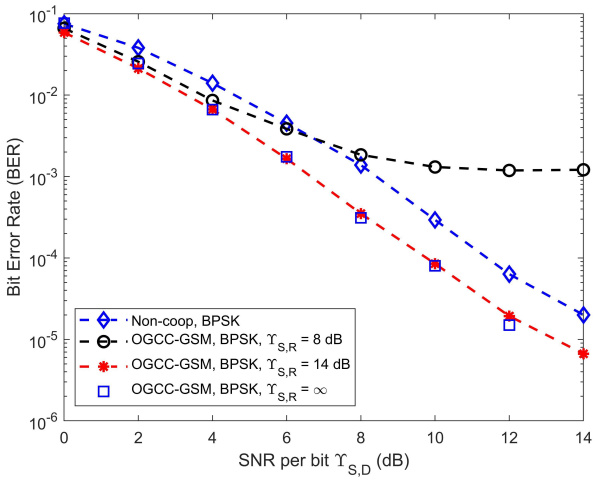

Fig. 13. Performance of the non-cooperative scenario of OGCC-GSM scheme and the proposed scheme via several S-R links ($\Upsilon_{S,R}$ = 8 dB, $\Upsilon_{S,R}$ = 14 dB (practical) and $\Upsilon_{S,R} = \infty$ (ideal)) for Scenario 1.

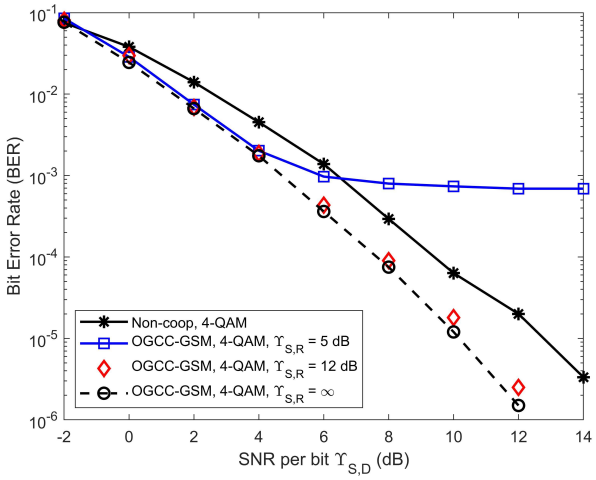

Fig. 14. Performance of the non-cooperative scenario of OGCC-GSM scheme and the proposed scheme via several S-R links ($\Upsilon_{S,R}$ = 5 dB, $\Upsilon_{S,R}$ = 12 dB (practical) and $\Upsilon_{S,R} = \infty$ (ideal)) for Scenario 2.

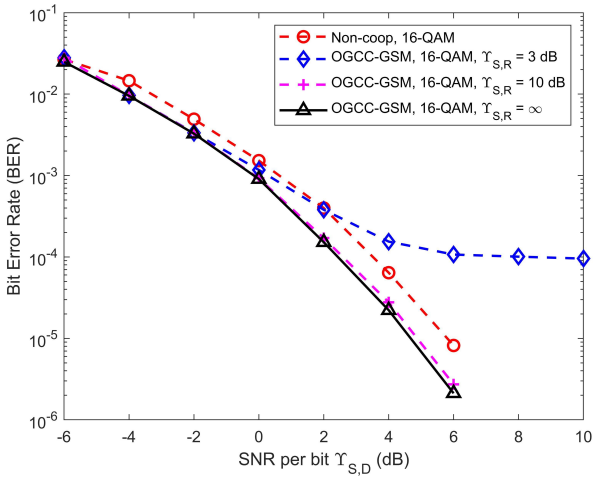

Fig. 15. Performance of the non-cooperative scenario of OGCC-GSM scheme and the proposed scheme via several S-R links ($\Upsilon_{S,R}$ = 3 dB, $\Upsilon_{S,R}$ = 10 dB (practical) and $\Upsilon_{S,R} = \infty$ (ideal)) for Scenario 3.

OGCC-GSM scheme. For example, when $\Upsilon_{S,R}$ = 3 dB, the BER curve of OGCC-GSM scheme for Scenario 3 becomes flat from SNR = 4 dB, which performs worse than the OGCC-GSM scheme under $\Upsilon_{S,R}$ = 10 dB by a margin of 7.5 dB at BER = 10^{-4}. And the performance curve of the OGCC-GSM under $\Upsilon_{S,R}$ = 10 dB almost coincides with that of the OGCC-GSM scheme under $\Upsilon_{S,R} = \infty$, as shown in Fig. 15. Therefore, the proposed OGCC-GSM scheme may achieve superior performance in practical application scenarios as the condition of the S-R channel is excellent. Moreover, from Figs. 13–15, the non-cooperative schemes of three scenarios all perform inferior to the cooperative scheme under the good S-R links by a margin of 2.2 dB loss at BER = 2×10^{-5} for Scenario 1, 3 dB loss at BER = 2.8×10^{-6} for Scenario 2, and, 1.6 dB loss at BER = 5×10^{-6} for Scenario 3, respectively. These simulation results further indicate that the relay that possesses more SNR than the source not only enables the coded cooperative scheme to achieve not only more coding gain through the use of the other Goppa code with more redundant symbols but also more diversity gain through the system structure of two paths compared to the non-cooperative scheme.

7.5 Performance of the OGCC-GSM Scheme Versus that of the Existing Schemes

In this subsection, the performance of the proposed OGCC scheme is first compared to that of the general LDPC coded cooperation [5] and the existing relay-optimized GCC schemes, i.e., the GCC scheme [9] and the jointly designed GCC scheme [10], shown in Fig. 16. Then, the BER performance curves of the existing DGC-SM schemes [17] and DGC-GSM [18] are also plotted in Fig. 16 to compare with that of the proposed OGCC-SM and OGCC-GSM schemes. For a fair comparison, the code rate $R_{CC} = 1/4$ is unified, and BPSK modulation and Rayleigh quasi-static fading are considered for all comparative schemes, where all simulated parameters of the proposed schemes refer to Scenario 1 of Tab. 5, and the good S-R link is set as $\Upsilon_{S,R}$ = 14 dB. Moreover, to keep the spectral efficiency consistent as 3 bits/s/Hz, determine $N_t = 4$, $N_r = 4$ for both the OGCC-SM scheme and its counterpart DGC-SM scheme, and $N_t = 4$, $N_a = 2$, and $N_r = 4$ for the OGCC-GSM and the comparative DGC-GSM schemes, respectively. Besides, the optimal TAC selection algorithm is utilized in both in both OGCC-GSM and DGC-GSM schemes.

From Fig. 16, the proposed OGCC scheme with the Patterson algorithm in each decoder outperforms the existing GCC schemes [9], [10] using the Euclidean algorithm and bit selection at the relay by a margin of over 4.2 dB at BER $\approx 2.8 \times 10^{-4}$. Although the proposed benchmark OGCC-SM scheme only obtains a gain of approximately 0.5 dB over the existing DGC-SM schemes [17] and DGC-GSM [18] at BER $\approx 5.6 \times 10^{-6}$, it avoids a significant amount of search caused by the relay information selection. Moreover, the proposed OGCC-GSM scheme performs substantially better than two comparable schemes under the same

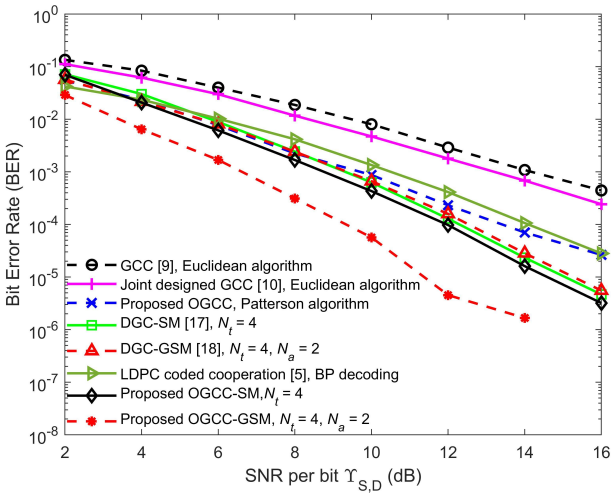

Fig. 16. BER performance comparison of proposed OGCC, OGCC-SM, and OGCC-GSM schemes with the existing LDPC coded cooperation, GCC, DGC-SM, and DGC-GSM schemes over the quasi-static Rayleigh fading channel, BPSK modulation, $R_{CC} = 1/4$.

spectral efficiency by more than 4.2 dB at BER $\approx 5.6 \times 10^{-6}$. In addition, the proposed scheme also outperforms the LDPC coded cooperation with the belief propagation (BP) decoding [5] by a gain of about 4.5 dB at BER $\approx 2.2 \times 10^{-5}$. In fact, the LDPC code is a kind of competitive channel code for large-scale information transmission due to its parallel iterative decoding algorithm based on the low-density sparse parity check matrix. However, in this comparison, short-length LDPC codes are used in the coded cooperation that demonstrates poor performance compared to the Goppa codes since the parity-check matrix of short LDPC codes is prone to short girths, which greatly affects the decoding performance. Therefore, in the small-scale information transmission, Goppa codes may be a stronger contender than the LDPC codes. The simulated results verify the effectiveness of selecting the Goppa polynomials for the Goppa codes in the overall system and further reveal the dominance of the proposed OGCC-GSM scheme.

8. Conclusion

This manuscript first investigates a simple but effective selection approach from the multiple Goppa polynomials to determine the optimal one that results in an optimized Goppa code with the largest MHD and the improved weight distribution. Based on this approach, two optimized Goppa codes with the same information dimension are distributed in the source and relay nodes, respectively, to construct the novel OGCC scheme where the Goppa code at the relay contains more redundant bits. To achieve more diversity gain, the OGCC-GSM scheme is proposed with more than one transmit antenna activated in comparison to its benchmark OGCC-SM scheme. Moreover, an RC-TAC selection algorithm is developed with the aid of CSI based on the existing optimal TAC selection algorithm. Additionally, a joint decoding approach is presented to further improve the system performance, where each decoder employs the novel Patterson algorithm. Numerical simulations evaluate the performance of the proposed OGCC-GSM scheme from different perspectives over the Rayleigh quasi-static fading channel, demonstrating the supremacy and feasibility of the proposed scheme. In the following work, we will focus on the more efficient joint decoding algorithm at the destination and consider the low-complexity relay symbol selection for the proposed scheme with different information dimensions.

Acknowledgments

This research is supported by the National Natural Science Foundation of China under the contract No. 61771241.

References

[1] XU, K., DU, Z. Y., JIANG, B. Dynamic coded cooperation with incremental redundancy: Throughput and diversity-multiplex tradeoff analysis. *IEEE Communications Letters*, 2020, vol. 24, no. 3, p. 506–509. DOI: 10.1109/LCOMM.2020.2969670

[2] HUNTER, T. E., NOSRATINIA, A. Diversity through coded cooperation. *IEEE Transactions on Wireless Communications*, 2006, vol. 5, no. 2, p. 283–289. DOI: 10.1109/TWC.2006.1611050

[3] ZENG, J. L., LIU, S.Y., WANG, H. Generalized distributed multiple turbo coded cooperative differential spatial modulation. *KSII Transaction on Internet and Information Systems*, 2023, vol. 17, no. 3, p. 999–1021. DOI: 10.3837/tiis.2023.03.017

[4] LIANG, H., LIU, A. J., LIU, X., et al. Construction and optimization for adaptive polar coded cooperation. *IEEE Wireless Communications Letters*, 2020, vol. 9, no. 8, p. 1187–1190. DOI: 10.1109/LWC.2020.2984738

[5] WANG, H., CHEN, Q. C. LDPC based network coded cooperation design for multi-way relay networks. *IEEE Access*, 2019, vol. 7, p. 62300–62311. DOI: 10.1109/ACCESS.2019.2915293

[6] ALMOLIKI, Y. M., ALDHAEEBI, M. A., ALMWALD, G. A., et al. The performance of RS and RSCC coded cooperation systems using higher order modulation schemes. In *Proceedings Sixth International Conference on Intelligent Systems, Modelling and Simulation*. Kuala Lumpur (Malaysia), 2015, p. 211–214. DOI: 10.1109/ISMS.2015.11

[7] GUO, P. C., YANG, F. F., ZHAO, C. L., et al. Jointly optimized design of distributed Reed-Solomon codes by proper selection in relay. *Telecommunication Systems*, 2021, vol. 78, no. 3, p. 391–403. DOI: 10.1007/s11235-021-00822-w

[8] LOPEZ, H. H., MATTHEWS, G. L. Multivariate Goppa codes. *IEEE Transactions on Information Theory*, 2023, vol. 69, no. 1, p. 126–137. DOI: 10.1109/TIT.2022.3201692

[9] WAWERU, D. K., YANG, F. F., ZHAO, C. L., et al. Design of optimized distributed Goppa codes and joint decoding at the destination. *Telecommunication Systems*, 2022, vol. 81, no. 3, p. 341–355. DOI: 10.1007/s11235-022-00948-5

[10] FENG, F. A., YANG, F. F., CHEN, C., et al. Jointly optimized design of distributed Goppa codes and decoding. *Radioengineering*, 2023, vol. 32, no. 1, p. 23–32. DOI: 10.13164/re.2023.0023

[11] CHEN, L., WANG, Z. Q., DU, Y., et al. Generalized transceiver beamforming for DFRC with MIMO radar and MU-MIMO communication. *IEEE Journal on Selected Areas in Communications*, 2022, vol. 40, no. 6, p. 1795–1808. DOI: 10.1109/JSAC.2022.3155515

[12] MESLEH, R. Y., HARALD, H., SINANOVIC, S., et al. Spatial modulation. *IEEE Transactions on Vehicular Technology*, 2008, vol. 57, no. 4, p. 2228–2241. DOI: 10.1109/TVT.2007.912136

[13] YOUNIS, A., SERAFIMOVSKI, N., MESLEH, R., et al. Spatial modulation. Generalised spatial modulation. In *Conference Record of the Forty Fourth Asilomar Conference on Signals, Systems and Computers*. Pacific Grove (USA), 2010, p. 1498–1502. DOI: 10.1109/ACSSC.2010.5757786

[14] BEZZATEEV, S. V., NOSKOV, I. K. Patterson algorithm for decoding separable binary Goppa codes. In *Wave Electronics and its Application in Information and Telecommunication Systems (WECONF)*. Saint Petersburg (Russia), 2019, p. 1–5. DOI: 10.1109/WECONF.2019.8840650

[15] XIAO, L. X., XIAO, P., XIAO, Y., et al. Transmit antenna combination optimization for generalized spatial modulation systems. *IEEE Access*, 2018, vol. 6, p. 41866–41882. DOI: 10.1109/ACCESS.2018.2859794

[16] MOON, J., PARK, J., LEE, J. Cyclic redundancy check code based high-rate error-detection code for perpendicular recording. *IEEE Transactions on Magnetics*, 2006, vol. 42, no. 5, p. 1626–1628. DOI: 10.1109/TMAG.2006.870444

[17] ZHAO, C. L., YANG, F. F., WAWERU, D. K., et al. Optimized distributed Goppa codes based on spatial modulation. *IET Communications*, 2023, vol. 17, no. 13, p. 1447–1464. DOI: 10.1049/cmu2.12634

[18] ZHAO, C. L., YANG, F. F., WAWERU, D. K., et al. Distributed Goppa-coded generalized spatial modulation: Optimized design and performance study. *Electronics*, 2023, vol. 12, no. 11. DOI: 10.3390/electronics12112404

About the Authors ...

Chen CHEN (corresponding author) was born in China. She received her B.S. degree in Electronic and Information Engineering from Yangzhou University, China, in 2020. She is currently doing the Ph.D. at the College of Electronics and Information Engineering, Nanjing University of Aeronautics and Astronautics, China. Her research interests are circuits and systems, signal processing, and channel coding.

Fengfan YANG was born in China. He received his M.Sc. and Ph.D. degrees from the Northwestern Polytechnical University and South-east University, China in 1993, and 1997, respectively, all in Electronic Engineering. He has been with the College of Information Science and Technology, Nanjing University of Aeronautics and Astronautics since May 1997. From October 1999 to May 2003, he was a research associate at the Centre for Communication Systems Research, University of Surrey, UK, and Dept. of Electrical and Computer Engineering, McGill University, Canada. His major research interests are information theory, channel coding, and their applications for mobile and satellite communications.

Daniel Kariuki WAWERU received his B.Sc. degree in Mathematics and M.Sc. degree in Pure Mathematics from the University of Nairobi, Kenya, in 2015 and 2017. He is currently doing Ph.D. from the College of Electronic and Information Engineering, Nanjing University of Aeronautics and Astronautics, China. His research interests are coding theory, information theory, channel coding for wireless communications.